Journal of Engineering and Technology for Industrial Applications

ISSN ONLINE: 2447-0228

ITEGAM-JETIA

Manaus, v.12 n.58, p. 47-52. March/April, 2026.
DOI: https://doi.org/10.5935/jetia. v12i58.2750

RESEARCH ARTICLE OPEN ACCESS

OPTIMIZATION OF PROCESS PARAMETERS FOR HORIZONTAL VIBRO-SEPARATOR WITH DYNAMIC MOTION ANALYSIS

Pavan Maheshchandra Bhatt*[1], D.H. Pandya[2]

[1]Research Scholar, faculty of Mechanical Engineering & Technology, Kadi Sarva Vishwavidyalaya, Gandhinagar,Gujarat, India.
[2]Professor, Department of Mechanical Engineering - LDRP-ITR , Kadi Sarva Vishwavidyalaya, Gandhinagar, Gujarat, India.

[1]http://orcid.org/0009-0004-1347-3226, [2]http://orcid.org/0000-0002-1619-6170

Email: *vpmppavan@gmail.com, veddhrumi@gmail.com

ARTICLE INFO

Article History
Received: September 27, 2025
Reviewed: January 19, 2026
Accepted: January 28, 2026
Published: March 31, 2026

Keywords:
Dynamic Motion analysis,
FFT,
Vibro-separator,
Poincaré,
CAE,
flow rate.

ABSTRACT

To optimize operating parameters, this paper conducted a dynamic motion analysis of a reciprocating vibro separator. This work examined the impact of motor speed and angle to determine the vibro separator's flow rate. For the dynamic motion analysis, a CAD model of the device was created using parametric software. Then, it was analyzed using a CAE tool at three distinct motor angles and speeds. Various motor angles (28°, 30°, and 32°) and speeds (1,000 RPM) were used in the dynamic motion investigations. In order to determine if a system is in periodic, quasi-periodic, multi-periodic, or chaotic motion, Poincaré maps, FFT (fast Fourier transform), and TDR (time-displacement response) were employed. A sensitivity-based uniaxial piezoelectric sensor was used to gather experimental data from the agriculture industry. Additional parameter changes were made to the computational model after computational studies were verified using real-time industrial data.The outcome of the present research leads us to conclude that the most suitable motor angle and speed for a horizontal vibro separator are 28° and 1050 RPM, respectively.

I. INTRODUCTION

In the modern industrial landscape, technology plays a key role in minimizing labor costs and delivering efficient solutions. One such technology is the vibro separator, a machine designed to remove impurities from materials while maintaining a high flow rate. The performance of the vibro separator is strongly influenced by its dynamic characteristics. To manage vibrations, industries commonly employ rubber dampers. Research efforts have particularly emphasized the damping properties of rubber. For instance, proposed an approach to optimize the design of rubber elastic dampers by analyzing their dynamic mechanical behavior [1]. By developed a dynamic model for a rubber isolator by combining hyper elastic, viscoelastic, and elastoplastic models and forecasting the relationship between the vibration isolator's amplitude and frequency [2].

A recent study highlights the influence of altering the motor angle (α) and motor speed, while keeping other parameters unchanged, on the performance of a vibro separator. In this work, both experimental results and computational simulations are compared by systematically varying the motor angle (α) and motor speed. In this study, a computational model was created using parametric software. This computational model is validated using an existing industrial model based on input parameters such as the vibro motor angle (α), motor speed, and stiffness of the rubber pad. The dynamic failure of this computational model is checked for output parameters such as amplitude, dynamic motion behaviour, and velocity acceleration [3]. After the model is validated, the motor angle (α) and the speed of the vibro separator will be changed, and output data such as amplitude, dynamic motion behaviour, and flow rate will be gathered.

II. LITERATURE REVIEW

Propose a new type of vibrating screen that moves in a swing trace rather than a traditional linear motion, inspired by the motion of manual sieving for better screening performance [4]. Examined how pressure and temperature affect spring materials while considering static stiffness. This study assessed the connection between Young's modulus and rubber temperature, determining a quantitative correlation between the two.

Ultimately, the convexity correction method was found to be a more precise means of evaluating the static stiffness of a spring than the ellipse approximation method [5]. Proposes a new and improved structural design for vibrating screens that operate under very high loads (large material mass, strong vibrations, and harsh working conditions) [6]. Investigated the movement of the screen and determined that particle travel speed is highest during linear screening. They found that elliptical motion has better velocity and efficiency than other types of motion. Circular movement provides minimal velocity while maximizing screen efficiency [7]. Identified improved parameters for positioning the vibro motor to enhance the efficiency of the vibro screen. Their research analyzed different motion patterns, mainly classified as linear, circular, or elliptical.

The study focused on the placement of the exciter or vibro motor in relation to the screen's center of gravity. Based on this analysis, an optimized vibro screen design was proposed, which increases production rates without requiring additional power consumption [8]. Developed physical model to predict the transport velocity of a bed of crushed rock material moving along a vibrating screen with a circular stroke—an important parameter for understanding and optimizing screening performance such as bed thickness and capacity [9]. Explored the impact of vibro screen frequency and swing declination angle using DEM 3D simulations. Their research found that optimizing the frequency and corresponding angle of declination enhanced the simulated results of the vibro screen. The researchers proposed several empirical formulas through regression analysis as a final observation [10].

Investigates how vibration affects bulk granular materials, focusing on the dynamics of particle beds in industrial equipment like vibrating screens, feeders, and conveyors [11]. The researchers concluded that banana screening is more effective when the SDI increment is maintained between 100 and 50 [12], [13]. O paper investigates structural failure and sensitivity of a reconfigurable vibrating screen (RVS) used in mineral processing. The aim is to identify weak points, understand how different load conditions affect stress distribution, and propose design improvements.[14].The study explored the optimal operating speed of the vibro motor, identified within the range of 900–1,100 RPM, along with a separator box inclination of 5° relative to the horizontal. Monica Solding supported these findings by applying the Monte Carlo simulation technique for parameter optimization [9].

III. METHODOLOGY

III.1 COMPUTATIONAL ANALYSIS

A 3D CAD model of the reciprocating vibro separator was developed using parametric software, as illustrated in Figure 1, and analysed with a CAE tool. The primary components of the reciprocating vibro separator include: (1) vibro motor, (2) connecting plate, (3) rubber pad, (4) separator box, and (5) unbalanced mass. For the analysis, a tetrahedral mesh configuration was applied to the entire model. The mesh used for Analysis purpose is called tetrahedral shape type Mesh. Coarse mesh size was kept of 120 mm for separator box and for remain part it's default. Box mesh was taken to analyses rubber pad in model which led to generate total 27840 elements for entire model & 2347 elements for model of rubber foundation. Real time boundary conditions were applied to perform random -vibration analysis. Total 10 nods taken to reduce proceeding time and closer approximation of result.

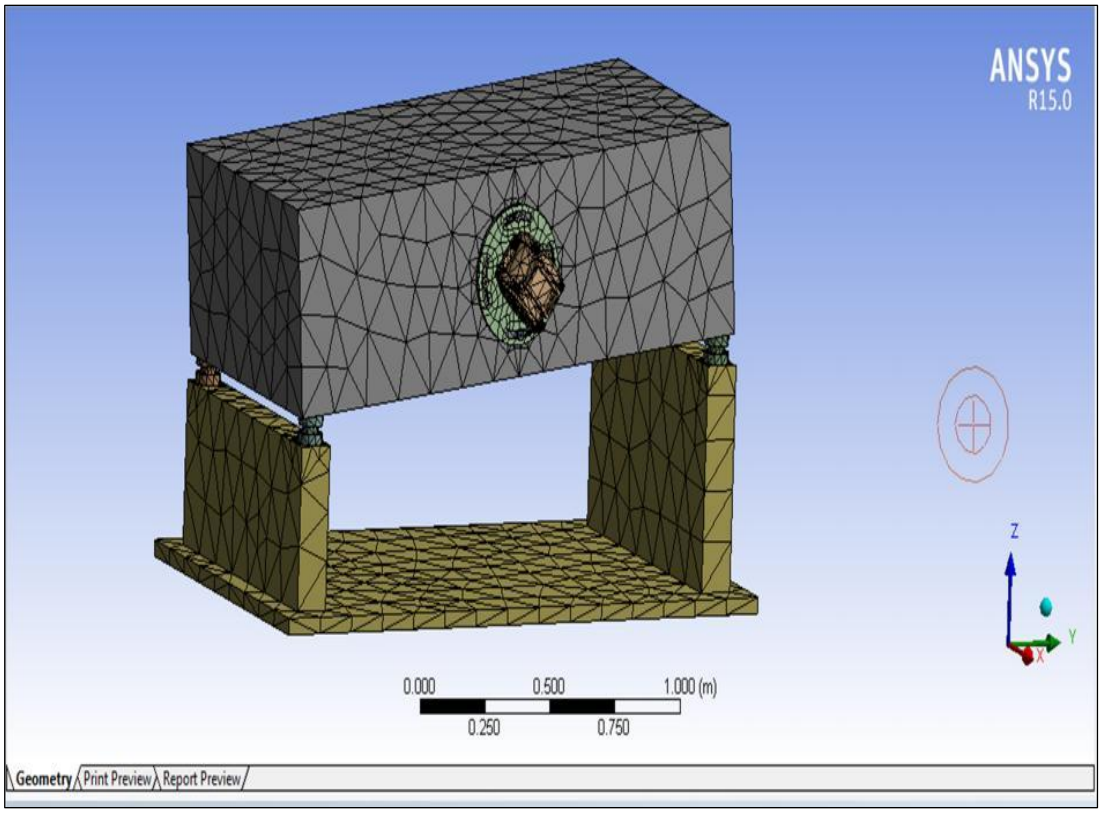

Figure 1: Parametric model of vibro separator.
Source: Authors, (2026).

Table 1: Effective Parameters of Reciprocating Vibro Separator.

Input Parameter	Output Parameter
Motor Angle (α)	Dynamic Motion Behavior
Motor Speed (RPM)	Amplitude, Flow rate
Foundation Rubber Properties	Flow rate

Source: Authors, (2026).

In this research work, From Table :1 Motor angle (α), Motor speed (RPM) are considered as a varying input parameter. For this varying input parameter, the dynamic motion behaviour and amplitude, flow rate is observed for Reciprocating vibro separator.

IV EXPERIMENTAL ANALYSIS

The experimental study was carried out at an operating speed of 1,000 RPM using two vibro motors, mounted on either side of the separator. Each motor had a power rating of 0.5 HP with a speed variation of ±20 RPM. Data acquisition was performed at GAJANAND Industries within the speed range of 980–1,020 RPM and at a motor angle of 30°. The detailed specifications of the experimental setup are presented in Table 2.

Table 2: Specification of reciprocating vibro separator.

Component	Weight (Kg)	Material
Separator Box	505.63	Structural steel
Plate	6.37	Structural steel
Foundation Rubber	0.335	Rubber
Each Motor without Unbalanced mass	35.91	Gray cat iron

Source: Authors, (2026).

Figure 2: Experimental Setup.
Source: Authors, (2026).

Real-time data was gathered from a vibro separator installed at Gajanand Industries, Siddhapur, Gujarat. As illustrated in Fig. 2, two vibro motors were mounted on opposite sides of the divider wall, each equipped with two unbalanced masses. The combined imbalance weight was measured at 3.34 kg. Data acquisition was performed at three distinct points on both sides of the separator. A uniaxial vibration sensor with a piezoelectric sensitivity of 1.02 mV/(m/s²) was employed, operating in IEPE input mode within the 1–10 kHz frequency range. The collected real-time data was subsequently analyzed and presented in a clear and accessible format

V. RESULTS AND DISCUSSION

From the Poincaré plots shown in Figure 2 for both experimental and computational results, it can be inferred that the computational model with a motor angle of 30°, a motor speed of 1,000 ± 20 RPM, and a foundation stiffness of 100 N/mm closely matches the behavior of the experimental vibro separator. Therefore, the computational model under these parameters demonstrates strong agreement with the experimental findings.

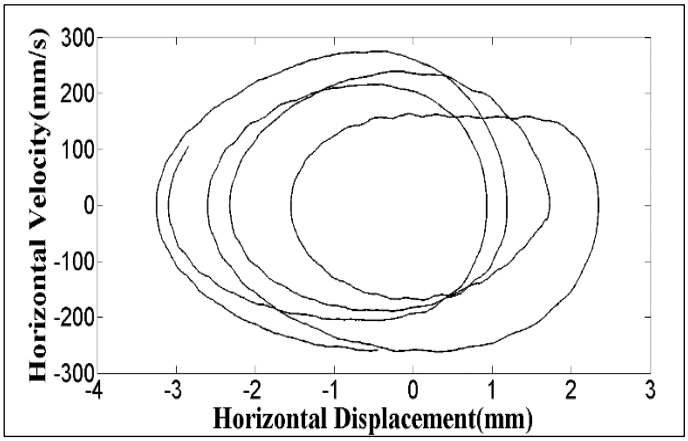

Figure 3(a): Computational Poincaré @ 100 N/mm stifness withHorizontal responses.
Source: Authors, (2026).

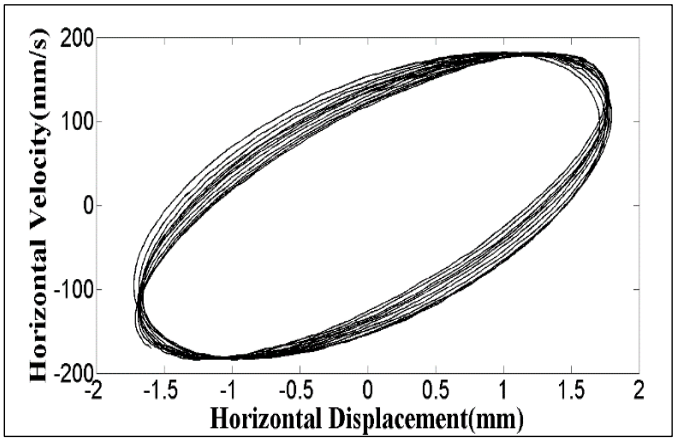

Figure 3(b): Experimental Poincaré @ 100 N/mm stifness with Horizontal responses.
Source: Authors, (2026).

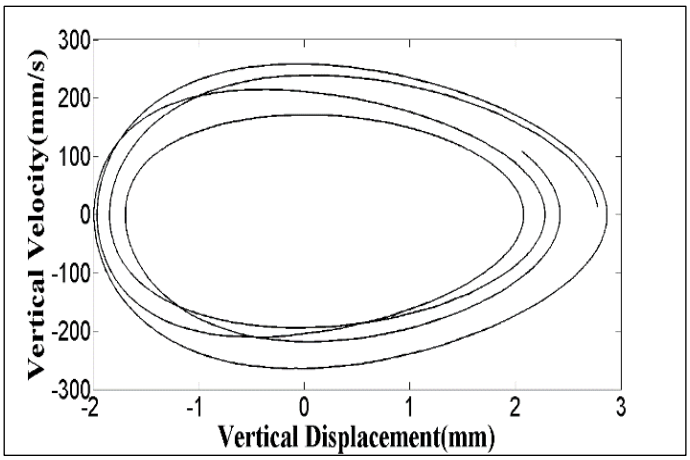

Figure 3(c): Computational Poincaré @ 100 N/mm stifness with Vertical responses.
Source: Authors, (2026).

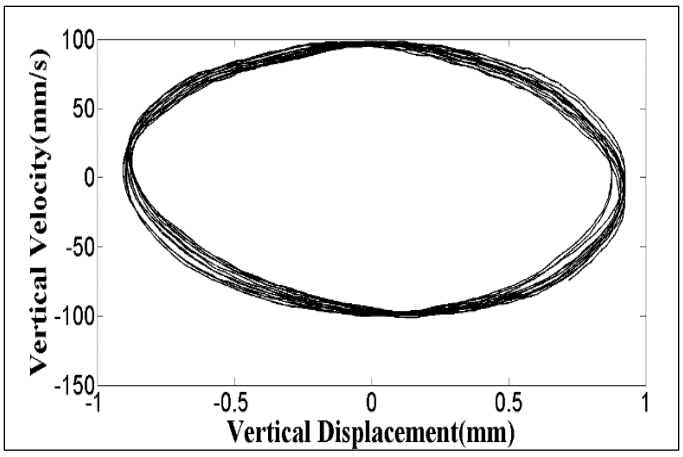

Figure 3(d): Experimental Poincaré @ 100 N/mm stifness with Vertical responses.
Source: Authors, (2026).

According to figure 3 (a-d) We verified the computational model by comparing the computational data with the experimental data and by looking at the TDR, FFT, and Poincaré chart. The validated computational model will use to achieve acceleration (mm/s2), displacement (mm), and velocity (mm/s2) for different motor angle (α), motor speed for both horizontal and vertical directions. The values are shown in Table3. As per Table 4 we are comparing the amplitude data for the different motor angle(α), with same motor speed(1000RPM) for better flow rate. Table 5 helps to compare the Dynamic motion behaviour with different Motor angle(α), with same motor speed(1000RPM).

Table 3: Computational data at different motor angle.

Angle (degree)	Speed (rpm)	Acceleration (mm/s^2)		Displacement(mm)		Velocity(mm/s^2)	
		Horizontal	vertical	horizontal	vertical	horizontal	vertical
28	1000	$-5.6X10^4$	$6X10^4$	-4.2	-4.3	-300.5	378
	1050	$3.9X10^4$	$4.5X10^4$	6.5	-6.4	300	-400
	1100	$-5X10^4$	$4X10^4$	-3.3	2.7	-200.9	200.5
30	1000	$2.8X10^4$	$1.5X10^4$	1.7	0.8	100.9	100
32	1000	$-5.6X10^4$	$3.9X10^4$	-6.8	6.6	-300.9	300
	1050	$3X10^4$	$-3.9X10^4$	-6.8	6.6	-300.9	300
	1100	$-5X10^4$	$1.5X10^4$	-4.3	-4.1	300.2	400

Source: Authors, (2026).

Table 4: Comparison of amplitude and dynamic motion behaviors data.

Data	Angle(degree)	Speed (rpm)	Amplitude (mm)	Dynamic motion
Computational	28	1000	4.5	Multi periodic
Computational	30	1000	1.75	Multi periodic
Computational	32	1000	4.3	Multi periodic

Source: Authors, (2026).

Based on study of above table no 4, we had found that motor angel 280 and 320 are optimized nearby value for better amplitude and effective dynamic motion behaviour. Amplitude value at motor angle 28° is higher than the motor angle 30° and 320. So, flowrate calculation is preferred for motor angle 28° compared to motor angle 300 and 32°. For flow rate calculations following equation is used which is mentioned in the equation 1.

$$\text{Flow rate of grain } (Q) = \rho * A * v \quad (1)$$

Here, it is assumed that grains are have uniform geometry which mean constant area and all grains are homogeneous in nature which led to conclude the constant density of grain. It means that velocity of grain flow is effective parameter to improve production rate of system. For calculating the flow rate computationally using different velocities for three different speeds as per table 3 use the equation mentioned as below as per equation 2. consider the flow rate experimentally as 4 tons per hour.

$$Q1/Q2 = V1/V2 \quad (2)$$

In above equation Q1 is flow rate of experimental, Q2 is flow rate of computational for different speed, v1 is velocity of grain at 300 angle and v2 is velocity of grain at 280 angles with three different speeds.

Table 5: Computational Data of Reciprocating Vibro Separator at 28º.

Angle (degree)	Speed(rpm)	Flow rate (tons per hour)	Dynamic motion
28	1000	14.99	Multi periodic
28	1050	15.86	Multi periodic
28	1100	7.9649	chaotic

Source: Authors, (2026).

As we know as the velocity increases the flow rate also increase but from the above Table 5 it has been observed that chaotic dynamic motion behaviour also plays vital role so at 280 angle and speed of 1100 the flow rate decreases. Hence at 280 angle and 1050 rpm the flow rate is maximum.

VI. CONCLUSION

In present work, a computational model has been developed for reciprocating vibro-separator. Dynamic motion analysis has carried out along with vibration responses of system. Overall computational data has validated with industrial data before proceed for further alteration. After validating computational model, significant parameters have altered to evaluate maximum flow rate with better dynamic motion of system. Hence major outcome of present work has concluded as follows:

(1) As per computational model analysis we had found higher amplitude when motor angle is 28^0 and 32^0. If we compare computational analysis and investigational data then we will get higher amplitude and better dynamic motion in case of motor angle 28^0 and motor speed 1000 rpm and 1050 rpm.

(2) The study reveals that the reciprocating vibro separator achieves a higher flow rate when operated at a motor angle of 28° with a speed of 1,050 RPM. Similarly, improved flow performance is also observed at the same motor angle (28°) with a motor speed of 1,000 RPM. The preferred motor speed is between 1000 and 1050 rpm as opposed to 1100 rpm, based on a higher flow rate at a motor angle of 28°. Additionally, analysis shows that the reciprocating vibro separator's flow rate is higher at motor angles of 28° than 30°.We will suggest the industry to set the motor angle 28^0 and motor speed 1000 or 1050 rpm to obtain the higher flow rate.

Present work will be useful for vibro-separator manufacturer to develop efficient and cost-effective product development. This work will be also useful for end user to operate present installed system with optimize parameters.

VII. AUTHOR'S CONTRIBUTION

Conceptualization: Pavan M Bhatt, Dr D H Pandya.
Methodology:. Pavan M Bhatt.
Investigation: Pavan M Bhatt.
Discussion of results: Pavan M Bhatt, Dr D H Pandya.
Writing – Original Draft: Pavan M Bhatt.
Writing – Review and Editing: Dr D H Pandya.
Resources: Pavan M Bhatt.
Supervision: Dr D H Pandya.
Approval of the final text: Pavan M Bhatt, Dr D H Pandya.

VIII. ACKNOWLEDGMENTS

The Green KSV Skill Development Centre in Gandhinagar provided assistance for the authors' experimentation and computational software tools.

IX. REFERENCES

[1] Lee, W.-S., Youn, S.-K., & Kim, B.-K. (2008). Finite element analysis and design optimization of rubber components for vibration isolation. Archives of Mechanics, 55(5-6), 449-479.

[2] Guo, X. Y., Zhou, J. Z., Feng, D. P., & Li, H. M. (2013). A method of calculating the dynamic characteristics of rubber isolator. Applied Mechanics and Materials, 395–396, 1170–1173. https://doi.org/10.4028/www.scientific.net/AMM.395-396.1170

[3] Jiang, H., Zhao, Y., Duan, C., Liu, C., Wu, J., Diao, H., Lv, P., & Qiao, J. (2017). Dynamic characteristics of an equal thickness screen with a variable amplitude and screening analysis. Powder Technology, 311, 239–246. https://doi.org/10.1016/j.powtec.2017.01.022

[4] Xiao, J., & Tong, X. (2013). Characteristics and efficiency of a new vibrating screen with a swing trace, Particuology, 11(5), 601–606. https://doi.org/10.1016/j.partic.2012.07.014

[5] Xu, C., Chi, M.-R., Dai, L., & Guo, Z. (2020). Calculation of nonlinear stiffness of rubber pad under different temperatures and prepressures. Shock and Vibration, 2020, Article ID 8140782. https://doi.org/10.1155/2020/8140782

[6] Baragetti, S. (2015). Innovative structural solution for heavy loaded vibrating screens, Minerals Engineering, 84, 15–26. https://doi.org/10.1016/j.mineng.2015.09.011

[7] Dong, H., Liu, C., Zhao, Y., & Zhao, L. (2013). Influence of vibration mode on the screening process. International Journal of Mining Science and Technology, 23(1), 95–98. https://doi.org/10.1016/j.ijmst.2013.01.014

[8] He, X.-M., & Liu, C.-S. (2009). Dynamics and screening characteristics of a vibrating screen with variable elliptical trace. Mining Science and Technology (China), 19(4), 508–513. https://doi.org/10.1016/S1674-5264(09)60095-8

[9] Soldinger, M. (2002). Transport velocity of a crushed rock material bed on a screen. Minerals Engineering, 15(1–2), 7–17. https://doi.org/10.1016/S0892-6875(01)00192-3

[10] Xiao, J., & Tong, X. (2013). Characteristics and efficiency of a new vibrating screen with a swing trace. Particuology, 11(5), 601–606. https://doi.org/10.1016/j.partic.2012.07.014

[11] Golovanevskiy, V. A., Arsentyev, V. A., Blekhman, I. I., Vasilkov, V. B., Azbel, Y. I., & Yakimova, K. S. (2011). Vibration-induced phenomena in bulk granular materials. International Journal of Mineral Processing, 100(3–4), 79–85. https://doi.org/10.1016/j.minpro.2011.05.001

[12] Dong, H. L., Liu, C. S., Zhao, Y. M., & Zhao, L. L. (2012). Banana screening method and simulation of banana screening process using Discrete Element Method. Advanced Materials Research, 524–527, 949–952. https://doi.org/10.4028/www.scientific.net/AMR.524-527.949

[13] Liu Chusheng , Wang Hong , Zhao Yuemin , Zhao Lala, Dong Hailin (2013). DEM simulation of particle flow on a single deck banana screen. International Journal of Mining Science and Technology, 23, 273–277.

[14] Ramatsetse, B., Mpofu, K., & Makinde, O. (2017). Failure and sensitivity analysis of a reconfigurable vibrating screen using finite element analysis. Case Studies in Engineering Failure Analysis, 9, 40–51. https://doi.org/10.1016/j.csefa.2017.04.001.